TÜBİTAK

Turkish Journal of Medical Sciences

http://journals.tubitak.gov.tr/medical/

Research Article

Turk J Med Sci
(2013) 43: 441-447
© TÜBİTAK
doi:10.3906/sag-1205-27

Measurement of the in-air output ratio for high-energy photon beams used in radiotherapy

Murugan APPASAMY[1,2,*], Sidonia Valas XAVIER[1], Thayalan KUPPUSAMY[1], Ramasubramanian VELAYUDHAM[2]

[1]Medical Physics Division, Dr Kamakshi Memorial Hospital, Pallikaranai, Chennai - 600 100, Tamil Nadu, India

[2]Nuclear and Medical Physics Division, School of Advanced Sciences, VIT University, Vellore - 632 014, Tamil Nadu, India

Received: 10.05.2012 • **Accepted:** 16.08.2012 • **Published Online:** 29.05.2013 • **Printed:** 21.06.2013

Aim: To measure the in-air output ratio of a 15-MV photon beam using locally designed miniphantoms.

Materials and methods: Columnar and brass miniphantoms were designed locally to accommodate 0.6 cc and 0.13 cc ionization chambers. The in-air output ratio (S_C) was measured for square, rectangular, and wedged fields for 15 MV. The influences of the orientation of the miniphantom, miniphantom material, and chamber volume on S_C and the collimator exchange effect were also studied.

Results: The S_C measurements ranged from 0.944 to 1.0321 for the studied field sizes. The orientation of the miniphantom had no influence on S_C for the range of field sizes studied. The collimator exchange effect was found to be within 1.57%. The S_C increased with wedged field sizes and wedge angles due to greater attenuation and production of low energy scatters.

Conclusion: This study suggests the combination of a polymethylmethacrylate miniphantom for larger field sizes and a brass miniphantom for smaller field sizes when measuring S_C in high-energy photon beams. The brass miniphantom with 0.6 cc and 0.13 cc ion chambers gives acceptable S_C values for small field sizes. The chamber volume (0.6 cc or 0.13 cc) has no impact when used with a brass miniphantom.

Key words: Head scatter factor, 15 MV, columnar miniphantom, collimator exchange effect

1. Introduction

Modern radiotherapy treatment planning systems use advanced model-based algorithms to achieve a high degree of accuracy with multileaf collimators (MLCs) and intensity modulation. To perform this, any algorithm should take into account different dose components of the beams like total scatter factor, head scatter factor, percentage depth dose, and beam profiles at different depths for different collimator settings. The in-air output ratio (S_C), also known as the head or collimator scatter factor for photon beams from megavoltage linear accelerators, describes the change of in-air output as a function of the collimator settings. The S_C depends on 1) collimator design, 2) scattering from the dose monitoring chamber, 3) scattering from the flattening filter, 4) the collimator exchange effect, and 5) beam-modifying devices (a physical wedge or a motorized wedge). Therefore, the accuracy of the dose-calculation algorithm indirectly depends on the correctness of the measured head scatter factor.

Several authors have investigated the measurement of head scatter factor, suitable materials for miniphantom design, and the depth of measurement. Kase and Svensson (1) measured the head scatter factor for several linear accelerators for the energy range of 4 to 24 MV using polystyrene and brass build-up caps. They reported a 5% variation of head scatter factor between linear accelerators, which was primarily due to the flattening filter. Huang et al. (2) studied the effect of collimator backscatter in the dose monitoring chamber of the linear accelerator for the energy of 4 to 15 MV, and they reported the effects to be negligible. The change of photon output with field size is predominantly due to the head scatter radiation. Van Gasteren et al. (3) were the first to report the measurement of head scatter factor using beam-coaxial narrow cylindrical phantoms. They measured the S_C at depths of 5 cm and 10 cm for quality indices of less than 0.75 and greater than 0.75, respectively. Karlsson et al. (4) reported the measurement of S_C at depths of 1 and 10 cm using the miniphantom for beam energies of 4 and 20 MV. Chaney et al. (5) reported a Monte Carlo study of head scatter factor. Shih et al. (6) proposed a method for the calculation of head scatter factor for an arbitrary

* Correspondence: vrs_murugan@rediffmail.com

jaw setting. Li et al. (7) studied the influence of lateral electron equilibrium and electron contamination in the head scatter factor measurement. Kim et al. (8) validated the equivalent square field formula for determining the S_C for rectangular fields. Douglas et al. (9) studied the head scatter factor measured with a miniphantom designed with different atomic numbers and at different depths. Zhu et al. (10) investigated the head scatter factor for small fields. Jursinic (11) reported different materials for the design of columnar miniphantoms, build-up caps, and S_C for 4, 10, and 18 MV photon beams. Venselaar et al. (12) reported the influence of electron contamination on the head scatter factor measurement and the importance of measuring at depths other than D_{max}, and they derived a relationship for converting the head scatter factor measured at D_{max} into the reference depth. Heukelom et al. (13) investigated the influence of wedges on in-air output ratio measurements with polymethylmethacrylate (PMMA) and brass build-up caps.

Though head scatter factor reference values are available in the literature, it may vary with individual linear accelerators, and the design of the collimator has an impact on high-precision treatment like intensity-modulated radiation therapy and image-guided radiation therapy. Therefore, an attempt is made here to measure the head scatter for a 15-MV photon beam using locally designed columnar and brass miniphantoms.

2. Materials and methods

2.1. Design of miniphantoms

In this study, PMMA is used in the fabrication of the columnar miniphantom. PMMA is a water-equivalent material $(C_2O_2H_8)_n$. It is cylindrical in shape and has a length of 18 cm, a diameter of 6.7 cm, and a wall thickness of 3 cm. The miniphantom has a stand made up of PMMA (density of 1.16 g/cm^3) to position it in the measurement position with parallel and perpendicular orientations. Screws are provided to position the chamber as well as the miniphantom. The miniphantom is suitable for the measurement of S_C in a parallel orientation at a 10 cm depth by using the 0.6-cc ion chamber (Figure 1).

The brass (density of 8.4 g/cm^3) miniphantom is designed with a wall thickness of 6 mm and is uniform around both the 0.6-cc and the 0.13-cc chambers (Figure 2). The 0.6-cc brass miniphantom is 1.9 cm in diameter and 4.2 cm in height. The 0.13-cc brass miniphantom is 1.9 cm in diameter and 2.2 cm in height. Both brass miniphantoms are cylindrical in shape and capable of measuring S_C with parallel and perpendicular orientations.

The 15-MV photon beam from the Primus (Siemens Medicals Systems, USA) linear accelerator is used for this study. A farmer-type ion chamber FG65C (Scanditronix Wellhöfer, USA), having an outer diameter of 0.71 cm, and a CC13 (Scanditronix Wellhöfer), having an outer diameter of 0.6 cm with a Dose 1 (Scanditronix Wellhöfer) electrometer, were used for the measurement of charge collection.

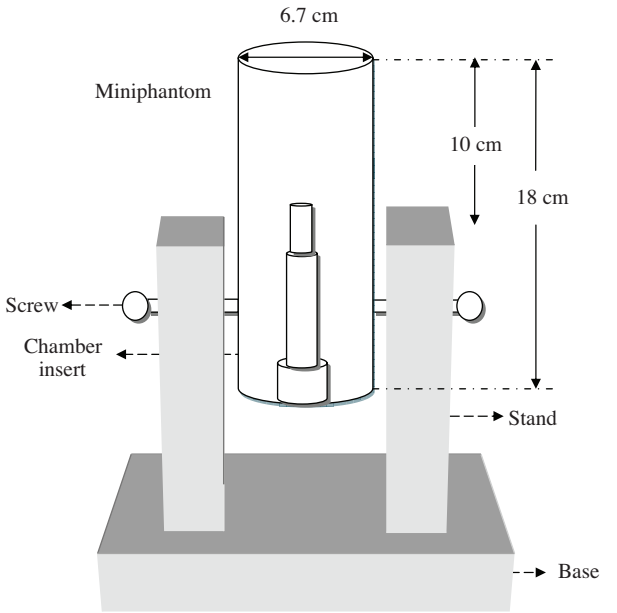

Figure 1. Design of the PMMA columnar miniphantom for a 15-MV photon beam.

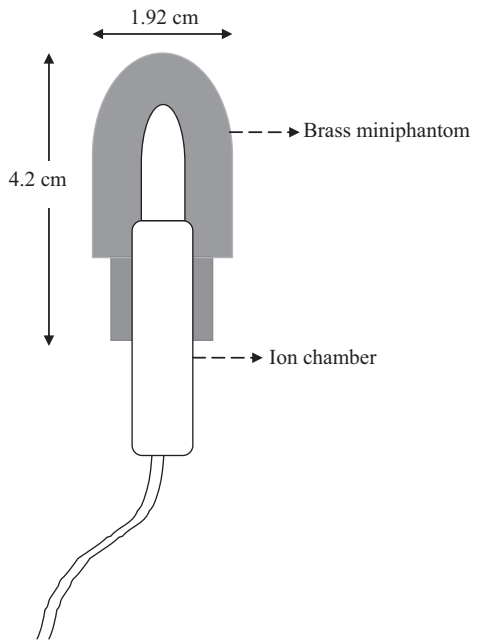

Figure 2. Design of the brass miniphantom for a 0.6-cc ion chamber.

2.2. Head scatter factor measurement

To measure the head scatter factor for 15 MV, the designed PMMA miniphantom was positioned in a stand parallel to the beam axis (Figures 3a and 3b) and the measurements were performed using a 0.6-cc ion chamber for field sizes from 3 × 3 cm^2 to 40 × 40 cm^2. The measurements were performed at a depth of 10 cm to avoid the uncertainty associated with electron contamination. When the outer dimension of the miniphantom (6.7 cm) approaches the field size at the isocenter (less than 8 × 8 cm^2), the S_C values become underestimated. In this situation, the field size is not fully covering the miniphantom and the scattering medium may not be constant. Jursinic (11) and Venselaar et al. (12) also suggested that S_C be measured at a depth of 5 to 10 cm to avoid electron contamination, and they suggested the use of high atomic number phantom material for smaller field sizes. Therefore, the measurements were carried out for small field sizes of 3 cm^2 to 10 cm^2 using the brass miniphantom with a 0.6-cc ionization chamber. The measurements were also performed using a brass miniphantom with a 0.13-cc ionization chamber to study the effect of chamber volume on S_C in smaller fields.

Measurements were carried out with parallel and perpendicular orientations to the beam axis with a source-to-chamber distance (SCD) of 100 cm. The measurements were also carried out for rectangular field sizes and for different wedge (physical wedge) angles. All the readings were measured for 100 MU (dose rate: 500 MU/min) with miniphantoms.

3. Results

Table 1 shows the head scatter factor measured in parallel orientation for the square (3 × 3 cm^2 to 40 × 40 cm^2) and rectangular field sizes (3 × 5 cm^2 to 30 × 40 cm^2) for a 15-MV photon beam measured using a PMMA miniphantom with a 0.6-cc ion chamber. The head scatter factors measured using a brass miniphantom with 0.6 cc for smaller field sizes are given with a superscript of (*). Similarly, the head scatter measurements using a brass miniphantom with 0.13 cc for smaller field sizes are given with a superscript of (^).

Table 2 presents the measured S_C values for various square field sizes from 3 × 3 to 25 × 25 cm^2 with open and wedge fields (15°, 30°, and 45°). A PMMA miniphantom with a 0.6-cc ion chamber was used for all the field sizes. A brass miniphantom with a 0.6-cc ion chamber was used for the measurement of smaller field sizes and is indicated with a superscript of (*). In the case of a 60° wedge, measurements were only carried out up to the 20 × 20 cm^2 field size. The deviation between the open and wedge head scatter is given in the table as percentages for 15°, 30°, 45°, and 60° wedges.

The comparison of the head scatter factor with and without a wedge presents a maximum deviation of 1.89%, 2.78%, 6.12%, and 2.9% and a minimum of 0.19%, 0.47%, 0.62%, and 0.7% for the 15°, 30°, 45°, and 60° wedge angles, respectively. The results of the present study agree well with the results of Shih et al. (14).

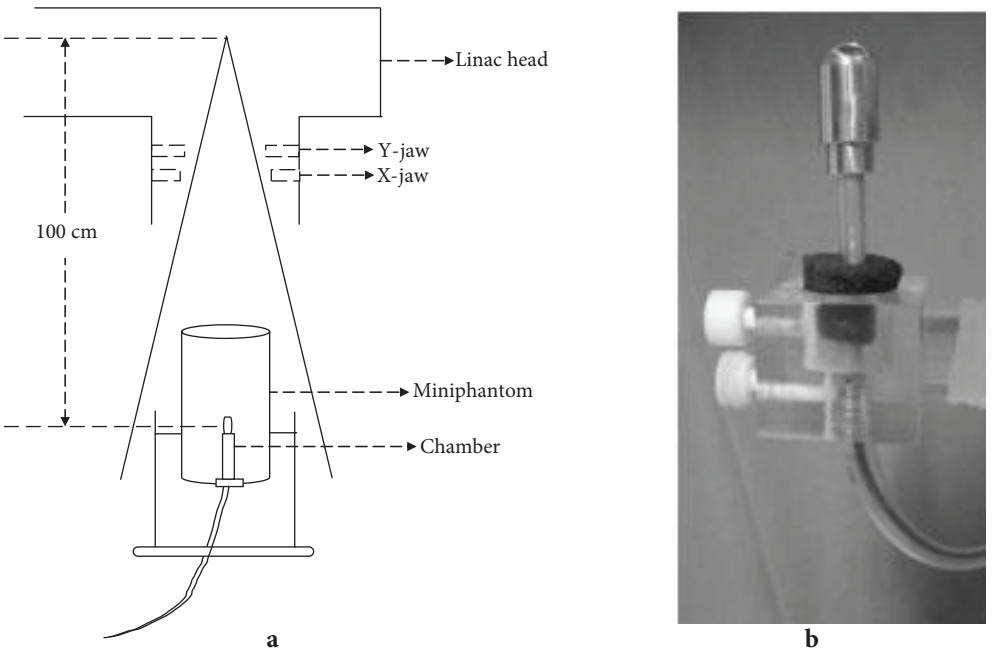

Figure 3. Designed PMMA miniphantom: a) experimental setup, b) brass miniphantom.

Table 1. Head scatter factor for square and rectangular field sizes for a 15-MV photon beam using 0.6 cc with a PMMA miniphantom.

Collimator setting (X/Y)	3	5	10	15	20	30	40
3	0.8660 0.9444 * 0.9487^	0.9047 0.9583* 0.9553^	0.9262 0.9734* 0.9721^	0.9317 0.9783* 0.9779^	0.9347 0.9800* 0.9823^	0.9360 0.9823* 0.9821^	0.9363 0.9840* 0.9836^
5	0.9009 0.9576* 0.9707^	0.9368 0.9662* 0.9678^	0.9736 0.9913* 0.9946^	0.9807 0.9989* 0.9995^	0.9837 1.0011* 1.0018^	0.9853 1.0040* 1.0023^	0.9864 1.0036* 1.0039^
10	0.9175 0.9649* 0.9671^	0.9668 0.9838* 0.9857^	1.0000 1.0000* 1.0000^	1.0158 1.0190^	1.0191 1.0239^	1.0207 1.0265^	1.0221 1.0273^
15	0.9197 0.9668* 0.9709^	0.9698 0.9851* 0.9875^	1.0095 1.0147^	1.0180	1.0253	1.0278	1.0299
20	0.9213 0.9666* 0.9710^	0.9720 0.9862* 0.9895^	1.0106 1.0132^	1.0237	1.0250	1.0302	1.0310
30	0.9221 0.9672* 0.9709^	0.9722 0.9847* 0.9891^	1.0120 1.0150^	1.0240	1.0294	1.0308	1.0286
40	0.9205 0.9651* 0.9704^	0.9728 0.9855* 0.9891^	1.0120 1.0161^	1.0250	1.0299	1.0316	1.0321

* represents the S_C measured with a 0.6-cc ionization chamber with a brass miniphantom; ^ represents the S_C measured with a 0.13-cc ionization chamber with a brass miniphantom.

Table 2. Head scatter factor for the wedged and open fields and the percentage of deviation.

Field size (cm^2)	Open field	15°	δ	30°	δ	45°	δ	60°	δ
3	0.9444*	0.9442*	0.02	0.9425*	0.20	0.9385*	0.63	0.9404*	0.42
5	0.9662*	0.9644*	0.19	0.9626*	0.38	0.9597*	0.67	0.9594*	0.70
8	0.9923*	0.9907*	0.15	0.9876*	0.47	0.9870*	0.53	0.9875*	0.48
10	1.0000	1.0000	0.00	1.0000	0.00	1.0000	0.00	1.0000	0.00
12	1.0095	1.0105	−0.10	1.0117	−0.22	1.0164	−0.68	1.0147	−0.51
15	1.0180	1.0221	−0.41	1.0239	−0.58	1.0362	−1.79	1.0314	−1.32
18	1.0234	1.0312	−0.76	1.0370	−1.32	1.0540	−2.99	1.0464	−2.25
20	1.0250	1.0370	−1.17	1.0424	−1.69	1.0660	−3.99	1.0547	−2.90
23	1.0270	1.0425	−1.51	1.0518	−2.42	1.0803	−5.19		
25	1.0278	1.0472	−1.89	1.0564	−2.78	1.0907	−6.12		

* represents head scatter factor measured using a brass miniphantom with a 0.6-cc ion chamber.

4. Discussion

The head scatter is measured with a locally designed miniphantom and validated by comparing the measured data with literature data. The physical origin of S_C is mainly due to the change in the amount of scattered radiation in the linear accelerator head as observed by the detector and to the change in the amount of backscatter radiation in the beam-monitoring chamber (10). The S_C values also vary with square, rectangular, and wedged fields and the exchange of collimator openings.

The measured head scattered factors with different orientations of the PMMA miniphantom with a 0.6-cc ion chamber and the data of Zhu et al. (10) are plotted in Figure 4. The head scatter factor measured in a parallel orientation is compared with the data od Zhu et al. (10), and it agrees within ±0.3% for all the field sizes except 3 × 3 cm², for which the deviation is found to be –2.7%. Similarly, the S_C values measured in a perpendicular orientation are compared with those of Zhu et al. (10); the deviation is found to be within ±1.15% and the corresponding deviation for a 3 × 3 cm² field size is +4.2%. The comparison of parallel and perpendicular orientations of S_C measurements presents a deviation of +1.3% in small field sizes and –0.71% in larger field sizes. This reveals that both parallel and perpendicular orientations account for the same amount of head scatter and that the orientation of the chamber has no influence on head scatter measurement.

To study the usefulness of brass miniphantoms for small field sizes, Figure 4 is redrawn with brass phantom values up to a 10 × 10 cm² field size and with PMMA miniphantom values above 10 × 10 cm² field sizes (in Figure 5) in parallel orientation. In the case of brass miniphantoms, both the 0.6-cc and 0.13-cc chamber measurements are included.

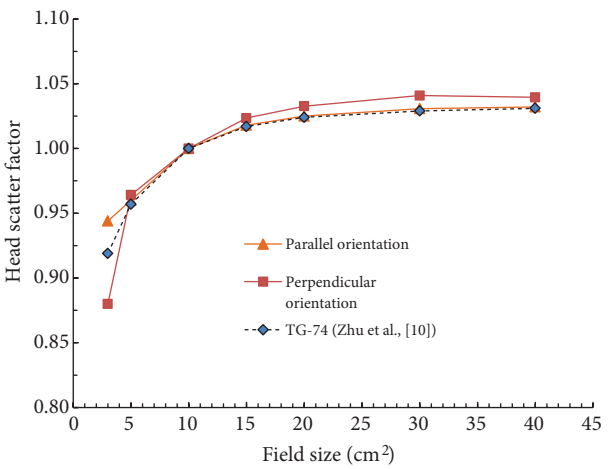

Figure 4. Head scatter factor for square fields using a miniphantom with a parallel and perpendicular orientation to the beam axis.

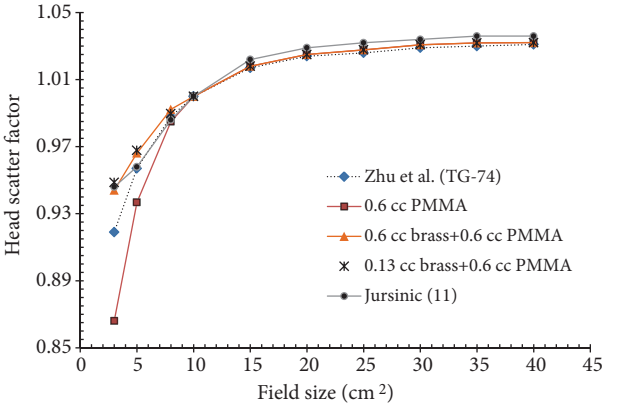

Figure 5. S_C measured with a brass miniphantom (0.6 cc and 0.13 cc) up to 10 × 10 cm² and a PMMA miniphantom with 0.6 cc for higher field sizes, compared with the literature data.

It was found that S_C values are consistent for all the field sizes above 10 × 10 cm² for both PMMA and brass miniphantoms. The PMMA miniphantom with a 0.6-cc chamber underestimates the S_C values for field sizes of less than 10 × 10 cm².

The analysis of the S_C values measured in smaller field sizes with a brass miniphantom with a 0.6-cc ion chamber and a brass miniphantom with a 0.13-cc ion chamber are in good agreement with the findings of Zhu et al. (10), with an accuracy of +2.7%. This indicates the usefulness of brass miniphantoms for smaller field sizes. However, the brass miniphantoms with a 0.6-cc ion chamber and the brass miniphantoms with a 0.13-cc ion chamber predict more or less the same head scatter even for smaller fields. This reveals that the use of a brass miniphantom is very important for smaller field sizes, irrespective of whether the ion chamber volume is 0.6 cc or 0.13 cc.

The comparison of Jursinic's (11) data with the present brass phantom study reveals a good agreement (Figure 5) with an accuracy of 2.2% for the entire range of field sizes. Though Jursinic used PMMA material for the phantom, there is a one-to-one correspondence between his PMMA data and the present brass miniphantom. This may be due to the smaller PMMA miniphantom wall thickness (1.15 cm) that the present study has used.

The measured head scatter factor values for rectangular fields are compared with that of Zhu et al. (10) and a deviation of –5.2% is observed for a PMMA miniphantom with a 0.6-cc ion chamber (Table 1) for field sizes of less than 8 cm², whereas it agrees within ±0.8% with TG-74 data for field sizes greater than 8 cm². In the case of the brass miniphantom, deviations of –0.61% and –0.06% were observed for the 0.6-cc and the 0.13-cc ion chambers, respectively. This again suggests the usefulness of small-volume ion chambers for rectangular field sizes, and especially for smaller field sizes.

The collimator exchange effect on head scatter reveals that the head scatter varies with the openings of the X and Y jaws (Figure 6). Whenever there is a large change in the upper jaw opening (the Y jaw), the head scatter is found to be higher. The Y jaw is closer to the dose monitoring chamber, which causes large variations in the output, and the same is reflected in the head scatter measurement irrespective of the miniphantom and the volume of the chamber. The above increase may be due to the backscatter from the dose monitoring chambers. The collimator exchange effect is found to be less than 0.85% in larger field sizes (greater than 10 × 10 cm^2) and 1.57% in smaller field sizes. Ding (15) studied the collimator exchange effect and reported that the beam monitoring chamber is the cause for higher head scatter, which accounts for 50% of the backscatter. The present study also supports the above statement; however, the magnitude of head scatter due to the dose monitoring chamber is not the topic of interest here.

The plot of the head scatter factors for different wedges is compared with open fields in Figure 7. It reveals that the head scatter factor of the open field and of the wedged fields agrees very well for all the field sizes from 3 × 3 cm^2 to 10 × 10 cm^2, with an accuracy of 0.7%. However, it increases from the open field for higher field sizes above 10 × 10 cm^2, suggesting higher head scatter for larger fields with a wedge. It also reveals that the head scatter factor increases with the increase of wedge angle, except for the 45° wedge. The physical wedge attenuates both primary and scatter and also produces low energy scatters (15). Higher wedge angles offer greater attenuation with higher head scatter. In the case of a 45° wedge, the S_C is higher than that of a 60° wedge, which facilitates a longer path travel for 15 MV photons at the center of the wedge due to its specific design. Therefore, the attenuation and head scatter are not only different but also higher for a 45° wedge. The dimensions of the 45° and 60° wedges are shown in Figure 8.

In this study, the in-air output ratios were measured for the 15-MV photon beam of a Siemens (Primus) linear accelerator by using the locally designed PMMA and brass miniphantoms, and the results agree very well with the literature data. This study reveals that the orientation of the miniphantom has no impact on the head scatter factor measurement for the studied field sizes. The brass miniphantoms with 0.6-cc and 0.13-cc ion chambers give precise head scatter factor values for the smaller field sizes, especially those less than 10 × 10 cm^2. A chamber volume of either 0.6 cc or 0.13 cc has no impact when used with brass miniphantoms. This study also suggests the combination of PMMA miniphantoms for larger field sizes and brass miniphantoms for smaller field sizes when measuring S_C in high-energy photon beams, especially in

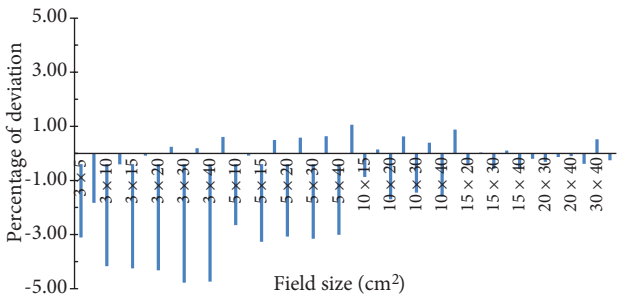

Figure 6. Percentage of deviation for the rectangular field sizes.

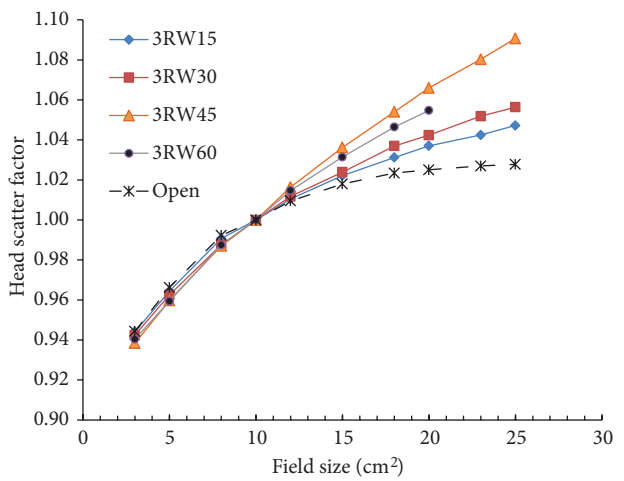

Figure 7. Head scatter factor for open and wedged fields in square fields for different wedge angles.

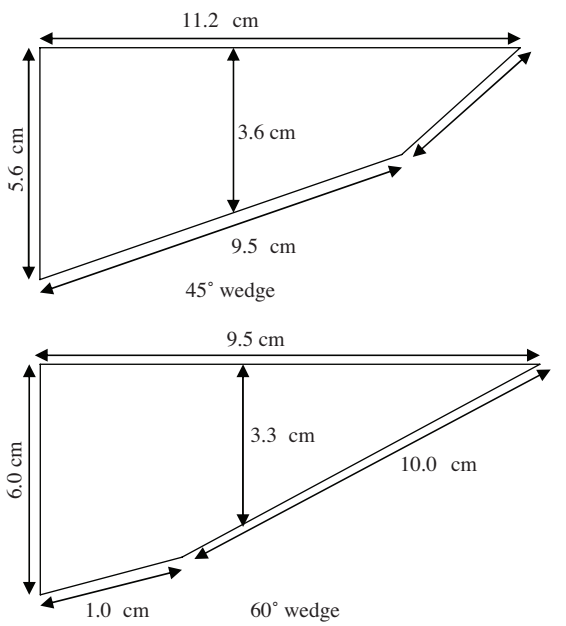

Figure 8. Physical dimensions of 45° and 60° physical wedges of Siemens Primus. The diagram is not to scale.

a 15-MV photon beam. The upper jaw (Y jaw) opening has a greater influence on head scatter due to the dose monitoring chamber backscatter, and it has influence on head scatter measurement, especially on the collimator exchange effect. The head scatter increases with wedged field sizes and wedge angles due to their greater attenuation and the production of low-energy scatters. This has a higher impact on a Siemens 45° wedge due to its specific geometric design.

Acknowledgement
We acknowledge the Managing Director of Dr Kamakshi Memorial Hospital for providing the facility to carry out this work. We also acknowledge medical physics team members Ms S Purnima, Mr TG Godwin Paul Das, and Ms Narmatha for their support.

References

1. Kase KR, Svensson GK. Head scatter data for several linear accelerators (4-18 MV). Med Phys 1986; 13: 530–2.
2. Huang PH, Chu J, Bjarngard BE. The effect of collimator backscatter radiation on photon output of linear accelerators. Med Phys 1987; 14: 268–9.
3. Van Gasteren JJM, Heukelom S, van Kleffens HJ, van der Laarse R, Venselaar JLM, Westermann CF. The determination of phantom and collimator scatter components of the output of megavoltage photon beams: measurement of the collimator scatter part with a beam-coaxial narrow cylindrical phantom. Radiother Oncol 1991; 20: 250–7.
4. Karlsson MG, Karlsson M, Sjogren R, Svensson H. Semiconductor detector in output factor measurements. Radiother Oncol 1997; 42: 239–96.
5. Chaney EL, Cullip TJ, Gabriel TA. A Monte Carlo study accelerator head scatter. Med Phys 1994; 29: 1383–90.
6. Shih R, Li XA, Chu JC, Hsu WL. Calculation of head scatter factor at isocenter or at center of field for any arbitrary jaw setting. Med Phys 1999; 26: 506–11.
7. Li XA, Soubra M, Szanto J, Gerig LH. Lateral electron equilibrium and electron contamination in measurements of head-scatter factors using miniphantoms and brass caps. Med Phys 1995; 22: 1167–70.
8. Kim S, Zhu TC, Palta JR. An equivalent square field formula for determining head scatter factor of rectangular fields. Med Phys 1997; 24: 1770–4.
9. Frye DM, Paliwal BR, Thomadsen BR, Jursinic P. Intercomparison of normalized head-scatter factor measurement techniques. Med Phys 1995; 22: 249–53.
10. Zhu TC, Ahnesjö A, Lam KL, Li XA, Ma CM, Palta JR et al. Report of AAPM Therapy Physic Committee Task Group 74: In-air output ratio, S_C, for megavoltage photon beams. Med Phys 2009; 36: 5261–91.
11. Jursinic PA. Measurement of head scatter factor of linear accelerators with columnar miniphantom. Med Phys 2006; 33: 1720–8.
12. Venselaar J, Heukelom S, Jager N, Mijnheer B J, van der Laarse, van Gasteren H et al. Effect of electron contamination on scatter correction factor for photon beam dosimetry. Med Phys 1999; 26: 2099–106.
13. Heukelom S, Lanson JH, Mijnheer BJ. Wedge factor constituents of higher energy photon beams: head and phantom scatter dose components. Radiother Oncol 1994; 32: 73–83.
14. Shih D, Li XA, Chu JC. Dynamic wedge versus physical wedge: a Monte Carlo study. Med Phys 2001; 28: 612–9.
15. Ding GX. An investigation of accelerator head scatter and output factor in air. Med Phys 2004; 31: 2527–33.